Chapter V: Structure and Magnetic Properties of $Ti_{1-x}Co_xO_{2-\delta}$ Thin Films Deposited by Pulsed Laser Deposition

This chapter deals with the structure and magnetic properties of $Ti_{1-x}Co_xO_{2-\delta}$ thin films deposited on Si and $LaAlO_3$ substrates using PLD technique under varying oxygen partial pressures. Oxygen partial pressure is maintained at 0 (vacuum), 0.1, 1 and 300 mTorr for $Ti_{1-x}Co_xO_{2-\delta}$ films deposited on Si substrate. For $Ti_{1-x}Co_xO_{2-\delta}$ films deposited on $LaAlO_3$ substrates, oxygen partial pressure is maintained at 0.1, 10 and 300 mTorr. The Co concentration in $Ti_{1-x}Co_xO_{2-\delta}$ films deposited on Si and $LaAlO_3$ substrates are 1.5 and 5 at % respectively. The possibility of secondary phase or presence of impurities on the magnetic properties is discussed. The probable role of defects like oxygen vacancies on crystal structure and magnetic properties has also been discussed.

5.1. Structure of $Ti_{1-x}Co_xO_{2-\delta}$ Thin Films Deposited on Si Substrate

Fig. 5.1 depicts the GAXRD pattern of TiO_2 thin films deposited on Si substrate under different oxygen partial pressures. The film deposited at vacuum does not correspond to either anatase or rutile phase of TiO_2 (denoted as '*' in Fig. 5.1). Rumaiz et al. (2007) observed similar unidentified peak at same diffraction angle deposited on Si substrate under vacuum condition. At 0.1 mTorr oxygen partial pressure, a broad peak centered at 26.7 ° is observed related to rutile phase of TiO_2. At 1 mTorr oxygen partial pressure, we observe anatase phase (A) with unidentified peak (denoted as '*' in Fig. 5.1) at $2\theta = 26.24^o$. This phase may be assigned to Ti_4O_7 phase (ICDD Card No: 77-1392). It has been formed due to the high degree of non-stoichiometry in the film as a consequence of oxygen deficiency during the film deposition. By careful investigation of the GAXRD pattern confirms the presence of this Ti_4O_7 phase (marked as *) in 0.1 mTorr deposited film. It is only merged in the broadness of the rutile (110) peak. At 300 mTorr oxygen partial pressure, all GAXRD peaks are matched well with the anatase phase of TiO_2 (ICDD Card No. 89-4921) contrary to the mixed anatase and rutile phase observed for the film deposited at 50 mTorr as demonstrated by Rumaiz et al. (2007). No other peaks have been evolved corresponding to any impurity phases within the detection

limit of our XRD. We reveal a gradual change in the phase from rutile to anatase with increasing the oxygen partial pressure from 0.1 to 300 mTorr (Fig. 5.1). However, it is not clear that why rutile phase is preferred at low and anatase at high oxygen partial pressures. The oxygen partial pressure dependence of phase has further been verified for Co-doped TiO_2 (CTO) thin films. Fig. 5.2 shows the GAXRD pattern of CTO films. Similar to TiO_2 film, we also observe Ti_4O_7 phase (marked as *) in CTO film deposited at vacuum. At 0.1 mTorr, though both films show rutile phase, the intensity of (110) peak is drastically enhanced. Further increasing the oxygen partial pressure to 1 mTorr, rutile phase persists in CTO film in contrary with the anatase phase in case of TiO_2 film. We observe anatase phase with a trace of rutile phase in the CTO film deposited at 300 mTorr oxygen partial pressure contrary to the complete anatase phase in case of TiO_2 film deposited at the same oxygen partial pressure.

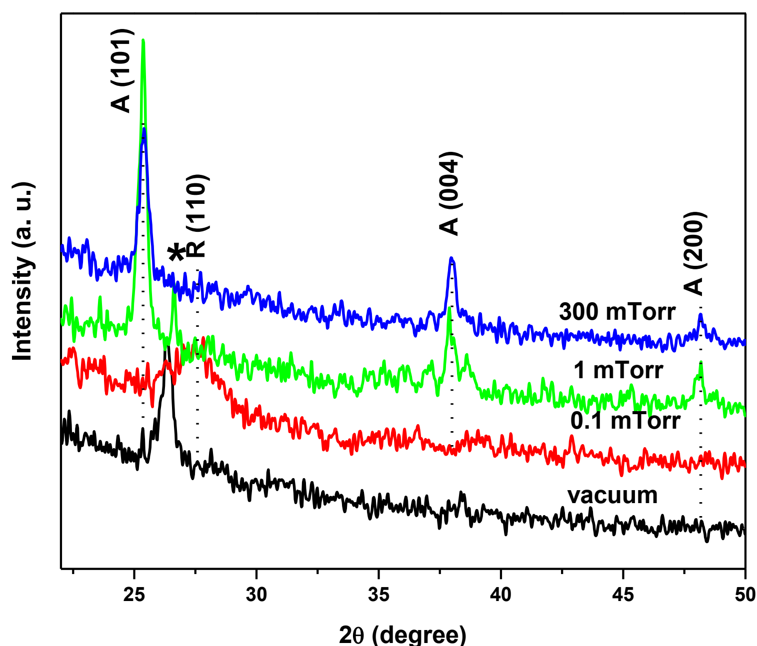

Fig.5.1. GAXRD pattern of TiO_2 thin films deposited at various oxygen partial pressures.

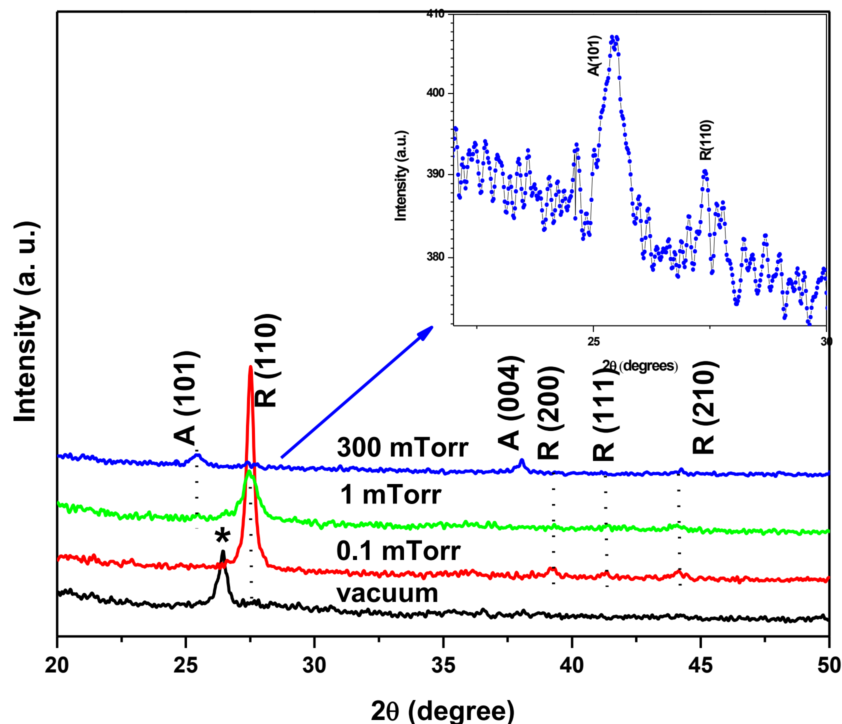

Fig.5.2. GAXRD pattern of CTO thin films deposited at various oxygen partial pressures. Inset shows the XRD spectrum of CTO film deposited at 300 mTorr oxygen partial pressure with 2θ = 20 - 30°.

The peak (110) corresponding to rutile phase is very small in comparison to the film deposited at 1 mTorr and is shown as inset of Fig.5.2. Although the GAXRD pattern for both TiO_2 and CTO films deposited under vacuum are same, a complete anatase phase in TiO_2 and a mixed (anatase and rutile) phase in CTO film deposited at 300 mTorr could be due to the cobalt substitution in TiO_2 matrix.

Fig.5.3 shows the Raman spectra of TiO_2 and CTO thin films which corroborate well with the XRD results. For instance, TiO_2 and CTO films deposited at oxygen partial pressure of 0.1 mTorr shows Raman A_{1g} mode at 612 cm^{-1} corresponding to pure rutile phase as observed from XRD. Similarly, in case of CTO film deposited at 300 mTorr oxygen partial pressure, we find E_g mode of anatase as well as A_{1g} mode of rutile phases. It has been reported that oxygen vacancy leads to the lattice distortion. Total energy calculations show

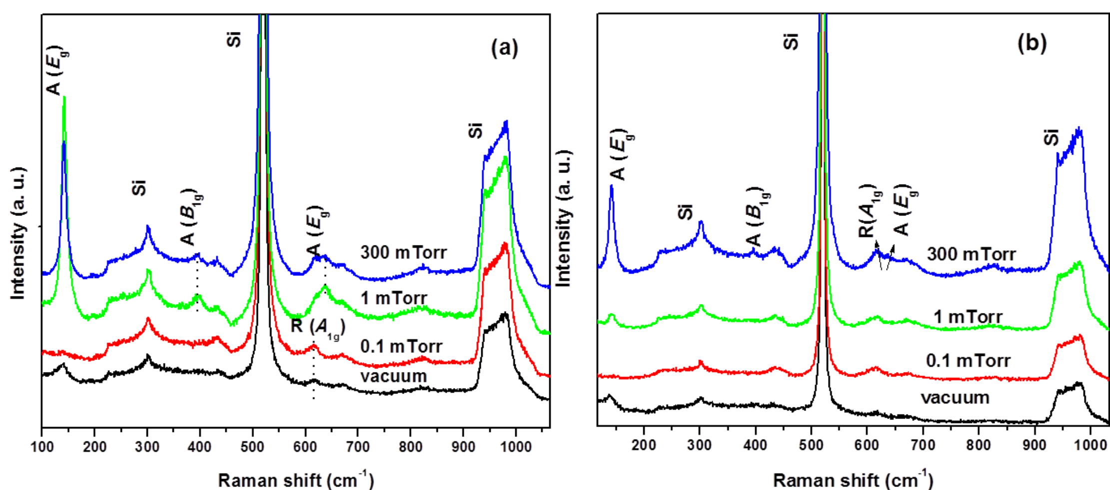

Fig.5.3 Raman spectra of (a) TiO_2 and (b) CTO films deposited at various oxygen partial pressures.

rutile phase to be more stable than anatase or brookite phase in such lattice distorted structure [Kim et al (2009)]. Therefore, as we increase the oxygen partial pressure, anatase phase forms due to decrease in oxygen vacancies in TiO_2 film. However, in CTO film deposited at 300 mTorr, the absence of complete anatase phase formation is due to higher oxygen vacancy compared to $TiO_{2-\delta}$ film. The thickness and composition of the films were measured using RBS. Simulation of the experimental data yields the exact thickness of the film. RBS plots of CTO films deposited at various oxygen partial pressures clearly indicate the presence of the elements Ti, O and Co (Fig.5.4). Black line represents the experimental data and the simulated spectrum is shown in red. The mismatch in the simulated and experimental curve at the Co edge suggests its non-uniform distribution in TiO_2 matrix. However, the average Co concentration in the film is found to be ~1.5 atomic percent. The film deposited at vacuum shows high degree of non-stoichiometry (O / (Ti+Co) ~ 1.2) which could be the reason behind the formation of Ti_4O_7 as observed from the GAXRD results. The calculated thickness and stoichiometry of the films are listed in the Table 5.1.

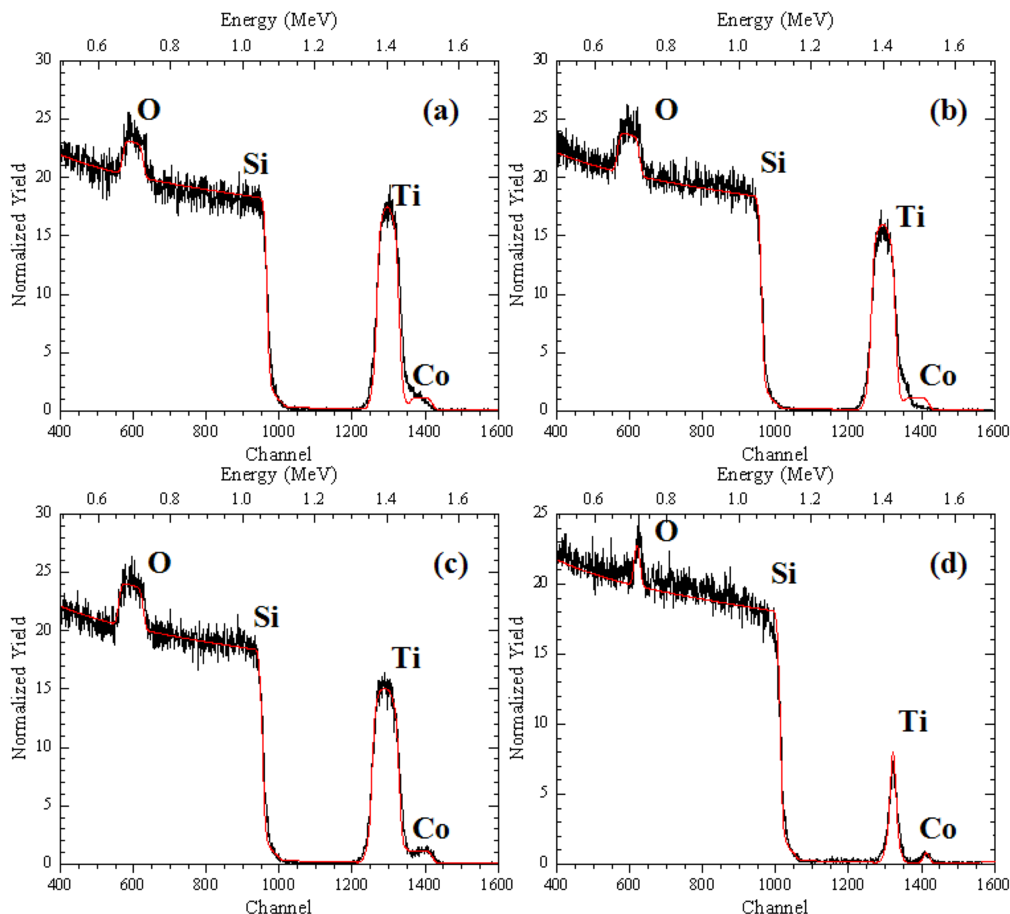

Fig.5.4. RBS spectra of CTO films deposited on Si: (a) vacuum, (b) 0.1 mTorr, (c) 1 mTorr and (d) 300 mTorr. Black line is the experimental data and the simulated spectrum is shown in red.

Table 5.1. Thickness and composition of $Ti_{0.985}Co_{0.015}O_{2-\delta}$ films deposited at various oxygen partial pressures.

O_2 Pressure	Thickness (nm)	Ti (at. %)	O (at. %)	Co (at. %)	O/(Ti+Co)
0 mTorr	135	43.9	54.5	1.6	1.2
0.1 mTorr	155	38.0	60.6	1.4	1.5
1 mTorr	178	35.0	63.5	1.5	1.7
300 mTorr	35	31.0	67.5	1.5	2.0

With increase in oxygen partial pressure, the stoichiometry of the films enhances. The thickness of the film is found to increase from 135 nm to 178

nm with increase in oxygen partial pressure from vacuum to 1 mTorr, and decrease abruptly to 35 nm in the film deposited at 300 mTorr oxygen partial pressure. The decrease in thickness of the film at 300 mTorr oxygen partial pressure is due to the presence of more oxygen in the chamber which acts as a barrier for the plume to reach the substrate and hence reduces the thickness of the film [Chrisey and Hubler (1994)]. Thus, the reduced XRD peak intensity in the above film could be due to the decrease in thickness.

Fig.5.5 shows the surface morphology of the CTO films with varying oxygen partial pressures. In vacuum, the surface is smooth and granular particles are uniformly distributed. Agglomeration is found to increase with increase in oxygen partial (Fig.5.5). Film deposited at 300 mTorr oxygen partial pressure shows randomly distributed micrometer sized particles over the film surface known as laser droplets (Fig.5.6).

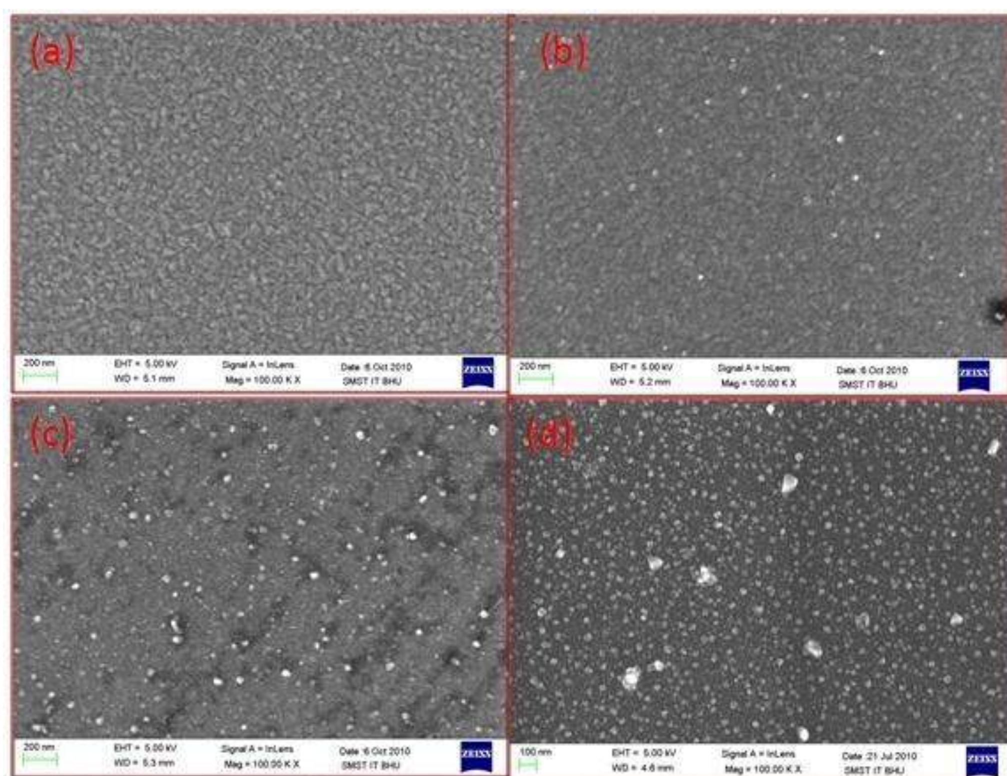

Fig.5.5 FE-SEM images of CTO thin film deposited at (a) vacuum, (b) 0.1 mTorr, (c) 1 mTorr, and (d) CTO 300 mTorr oxygen partial pressure.

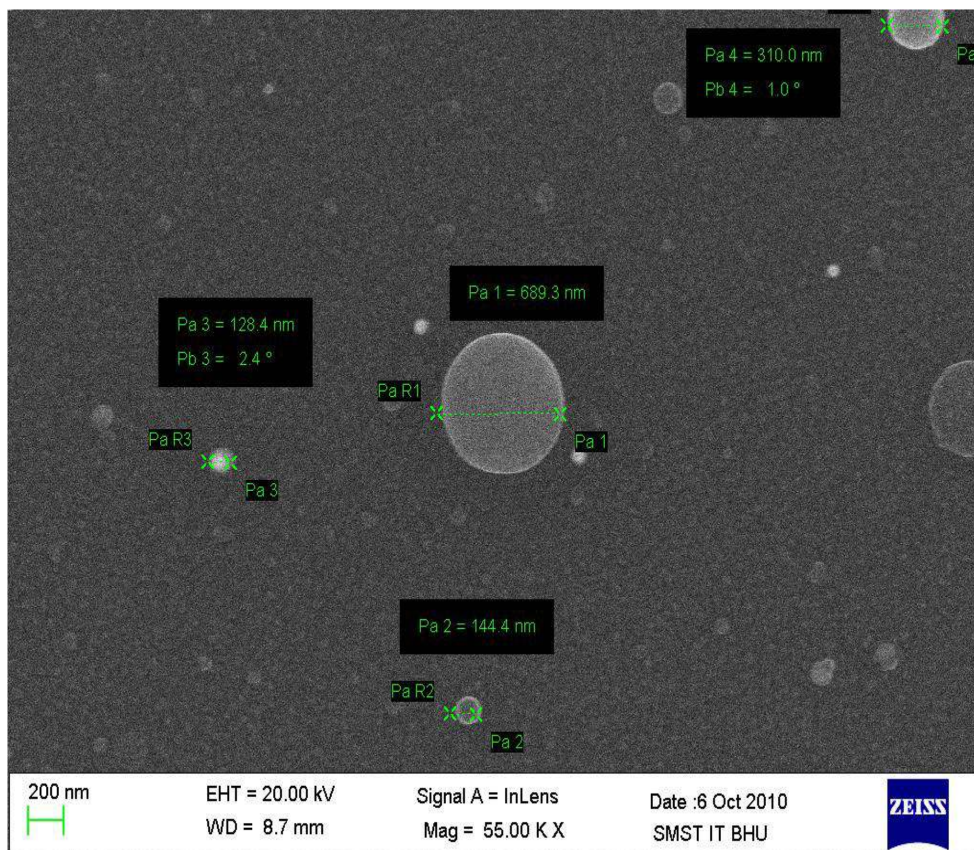

Fig.5.6 FE-SEM image of CTO thin film deposited at 300 mTorr oxygen partial pressure.

It is known that by doping lower valent ions like cobalt at titanium site, oxygen vacancies are created for charge neutrality and beyond a certain level of dopant concentration; phase becomes rutile [Hanaor and Sorrell (2011), Brakat et al. (2005)]. Thus, we believe that in CTO film deposited at 300 mTorr, the oxygen vacancies are more than in TiO_2 film (deposited at same oxygen partial pressure) and hence complete anatase phase formation is inhibited. XPS measurements further quantify the oxygen vacancy concentration in both films deposited at 300 mTorr oxygen partial pressure.

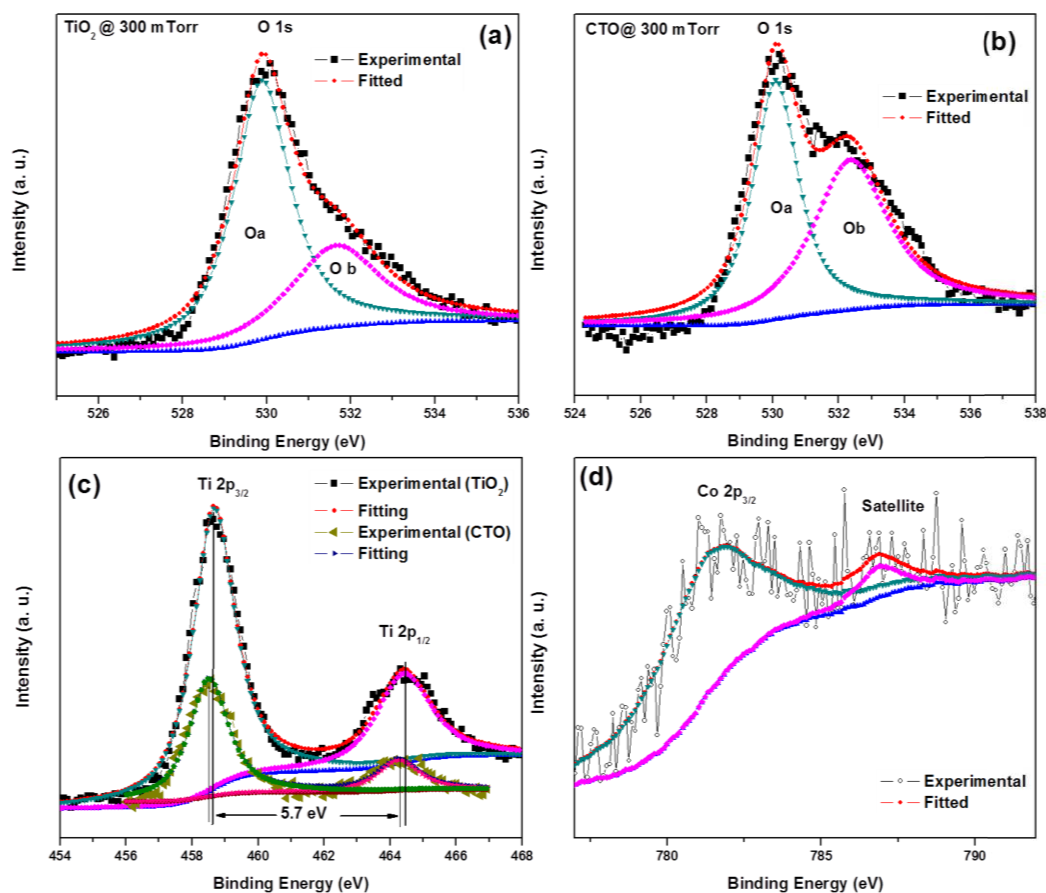

Fig.5.7. XPS core level spectra of: (a) O 1s level of TiO_2 ,(b) O 1s level of CTO film (c) Ti 2p level of TiO_2 and CTO film and (d) Co 2p level of CTO film deposited at 300 mTorr.

Fig. 5.7 (a) and (b) depict the O 1s core level peak of TiO_2 and CTO film deposited at 300 mTorr. The O 1s core level show a slightly asymmetric shape around 530 eV and are fitted with two symmetric Gaussian curves denoted as Oa and Ob peak respectively. The Oa and Ob peaks are ascribed to oxygen atoms of TiO_2 and hydroxyl groups, chemisorbed oxygen, and organic oxygen on the surface of the sample respectively [Rath et al. (2009). After comparing the area ratio of Ob to Oa in CTO as well as in TiO_2 film, it is observed that the area ratio is higher in CTO film than that of TiO_2 indicating the enhancement of oxygen vacancy concentration [Naeem et al. (2006)]. This supports our argument that CTO film has more oxygen vacancies than TiO_2 film grown under same condition. Fig.5.7(c) shows core level of Ti 2p spectrum of TiO_2 and CTO film respectively. The core level binding energy of

Ti $2p_{3/2}$ and Ti $2p_{1/2}$ in TiO_2 films are 458.6 and 464.3 eV, respectively. After incorporation of cobalt at Ti site, the peak positions of Ti $2p_{3/2}$ and $2p_{1/2}$ are found to be shifted towards lower binding energy (Fig.5.7 (c)). Similar peak shifting corresponding to Ti $2p_{3/2}$ and $2p_{1/2}$ has been observed by Sharma et al. (2011) and they have ascribed to the formation of defects like oxygen vacancies. However, the energy separation between Ti $2p_{3/2}$ and $2p_{1/2}$ of 5.7 eV in both films indicates a valence state of +4 for Ti [Rath et al. (2009)]. Fig.5.7 (d) shows the Co 2p core level spectrum. Due to low concentration of cobalt, the Co 2p region is not well resolved. However, after fitting, it shows a clear peak around 781 eV, which is higher than the binding energy reported for Co clusters [Shinde el al. (2003)]. The satellite like feature also confirms the bonding of Co with oxygen.

5.2 Structure of $Ti_{1-x}Co_xO_{2-\delta}$ Thin Films Deposited on $LaAlO_3$ Substrate

Fig.5.8 depicts the XRD pattern on $Ti_{1-x}Co_xO_{2-\delta}$ (x = 0.05) thin films deposited on $LaAlO_3$ substrate at varying oxygen partial pressures (0.1 mTorr, 10 mTorr and 300 mTorr). We have selected $LaAlO_3$ substrate as its lattice parameter resembles with the lattice parameter of anatase phase. The lattice mismatch (δ) is defined as:

$$\delta\% = \{(a_{substrate} - a_{film}) x\ 100\} / a_{substrate}$$

where a is the lattice parameter. Positive δ suggests in-plane tensile strain, while negative δ account for the in-plane compressive strain. The lattice parameter $LaAlO_3$ is 3.788 Å, whereas the lattice parameter for anatase TiO_2 is 3.785 Å, which results in a lattice mismatch of only 0.079%. Due to minimum lattice mismatch, all the films grow epitaxially along c direction [Kennedy and Stampe (2003)]. Also the anatase phase is retained in all the films with increasing oxygen partial pressure, contrary to the rutile phase formation in case of films deposited on Si substrate. For Si substrate δ is found to be 30% and 15% for anatase and rutile phases respectively. This may be one possible reason for the preference of rutile phase under low oxygen partial pressure in

case of films deposited on Si substrates. The reflections corresponding to (004) and (008) planes corresponding to anatase phase of TiO_2 are observed for the epitaxial films. Besides the major reflections marked as (001), (002) and (003), all reflections denoted as "s" correspond to $LaAlO_3$ substrate. With increase in oxygen partial pressure, the x-ray intensity decreases due to decrease in film thickness.

Fig.5.9 shows the XRD pattern of TiO_2 thin film deposited on $LaAlO_3$ substrate grown under different oxygen partial pressures (0.1 mTorr, 10 mTorr and 300 mTorr). Similar to Co-doped TiO_2 thin films, only anatase phase has formed under different oxygen partial pressure.

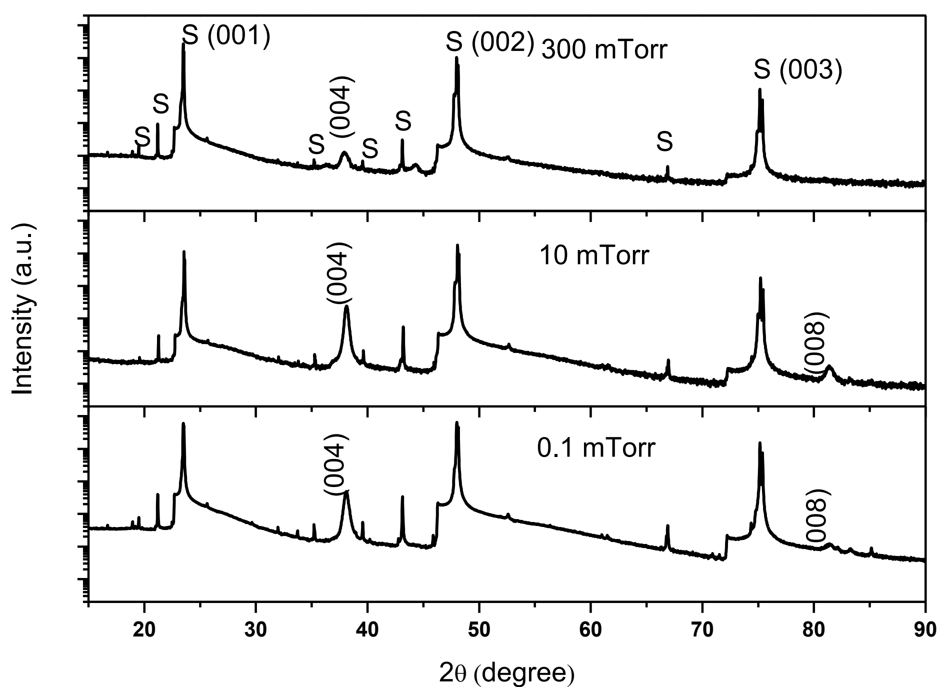

Fig.5.8 XRD pattern of $Ti_{0.95}Co_{0.05}O_{2-\delta}$ films deposited on $LaAlO_3$ substrate at different oxygen partial pressures.

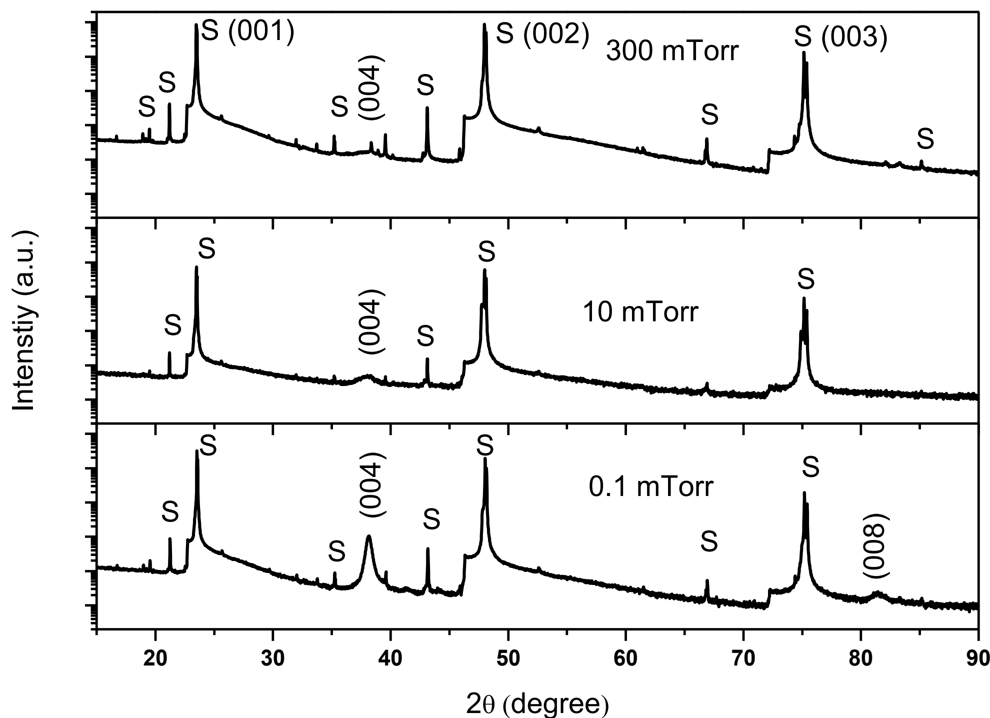

Fig.5.9 XRD pattern of $TiO_{2-\delta}$ films deposited on $LaAlO_3$ substrate at different oxygen partial pressures.

Raman spectroscopy has been carried out to confirm the structure of the films. The typical Raman spectra for TiO_2 and CTO films deposited on $LaAlO_3$ substrate at 0.1 mTorr oxygen partial pressure is shown in Fig. 5.10. Due to epitaxial nature of the films, the E_g mode (at 145 cm^{-1}) of anatase phase has been merged with the A_{1g} mode (at 123 cm^{-1}) of $LaAlO_3$ substrate (Fig. 5.10). Only B_{1g} mode appears around 400 cm^{-1} related to anatase phase of TiO_2. Besides A_{1g} mode related to $LaAlO_3$, the other two modes are denoted as E_{1g} and E_g as shown in Fig.5.10.

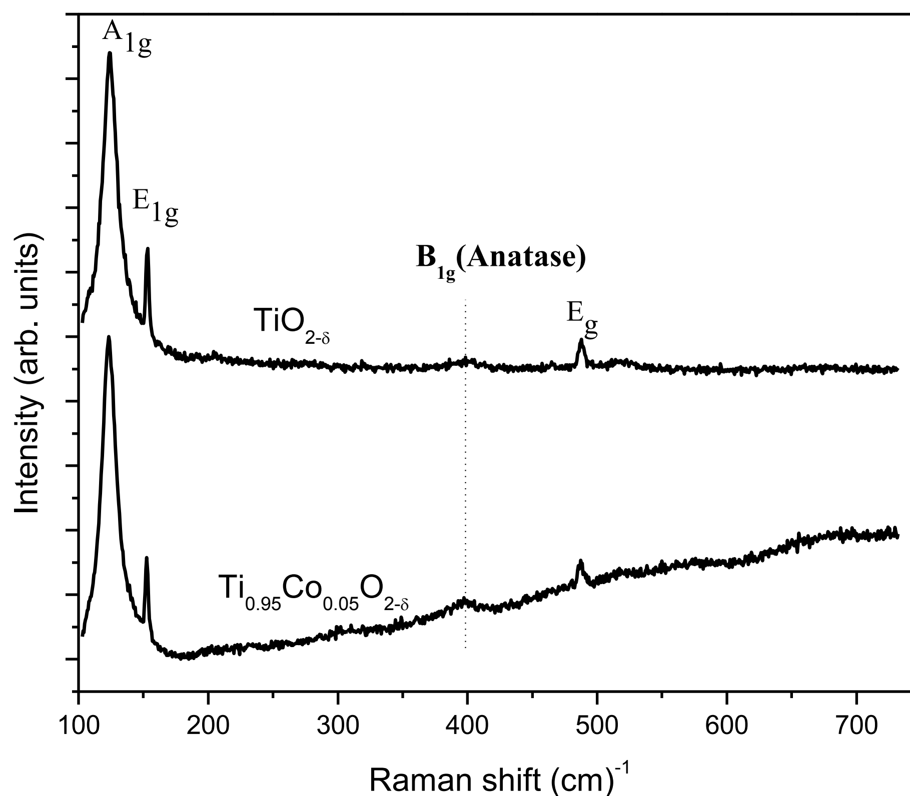

Fig.5.10 Raman spectra of $Ti_{1-x}Co_xO_{2-\delta}$ (x = 0, 0.05) films deposited at 0.1 mTorr oxygen partial pressure.

Fig. 5.11 shows typical RBS spectra of $Ti_{1-x}Co_xO_{2-\delta}$ film grown on $LaAlO_3$ substrate under 0.1 mTorr oxygen partial pressure. No element other than La, Ti, O and Co has been detected from RBS. The Co edge is not clear from the RBS due to its low concentration. RBS/channeling measurement of TiO_2 film deposited at 0.1 mTorr shows significant decrease in normalized yield in comparison to random case indicating the epitaxial growth of thin films (inset of Fig.5.18: black-random, red - channelling). Similar epitaxial growth of TiO_2 films on $LaAlO_3$ have been confirmed from ϕ scan measurements as reported in literature [Lotnyk et al. (2007)].

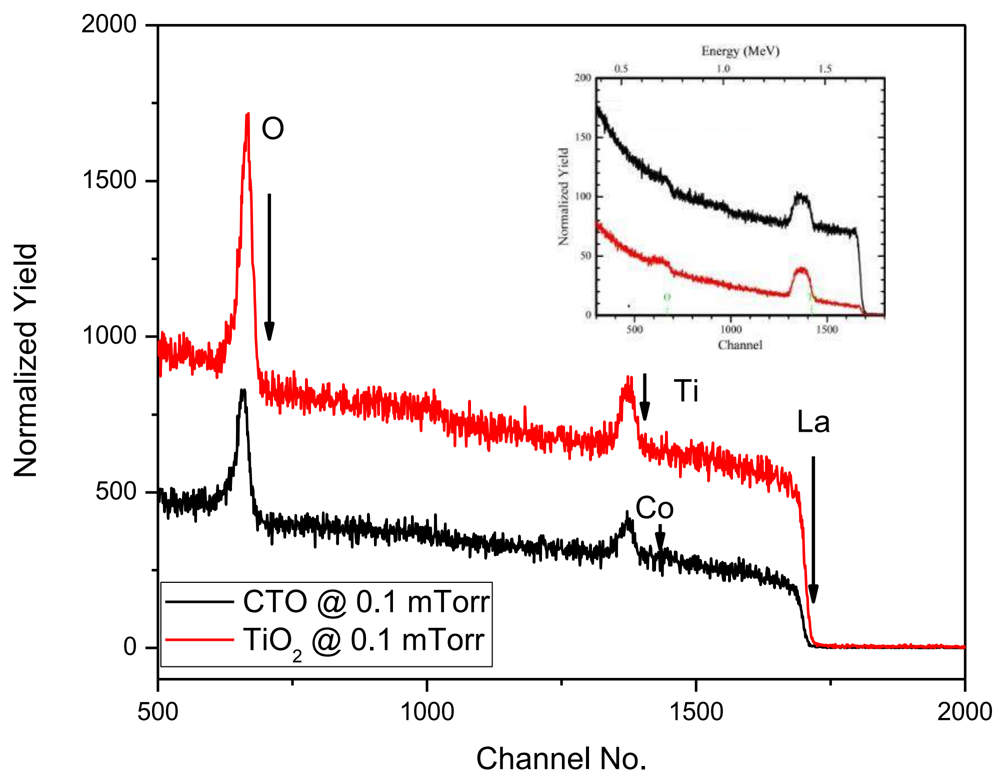

Fig.5.11 Oxygen resonance RBS result of $Ti_{0.95}Co_{0.05}O_{2-\delta}$ and $TiO_{2-\delta}$ film deposited on $LaAlO_3$ substrate at 0.1 mTorr oxygen partial pressure. The inset shows the RBS/channeling results for $TiO_{2-\delta}$ film.

The surface morphology of the CTO films with varying oxygen partial pressures (0.1, 10 and 300 mTorr) are shown in Fig.5.12 (a-c). The films are found to be composed of spherical nano-sized grains. The TiO_2 film deposited at 0.1 mTorr oxygen partial pressure show linear arrangement of the spherical grains (Fig.5.13). However, we could not resolve the surface morphology in TiO_2 thin films deposited at 10 as well as 300 mTorr oxygen partial pressure. From the SPM result, we can conclude that the as deposited films are crack free having uniform distribution grains over the substrate.

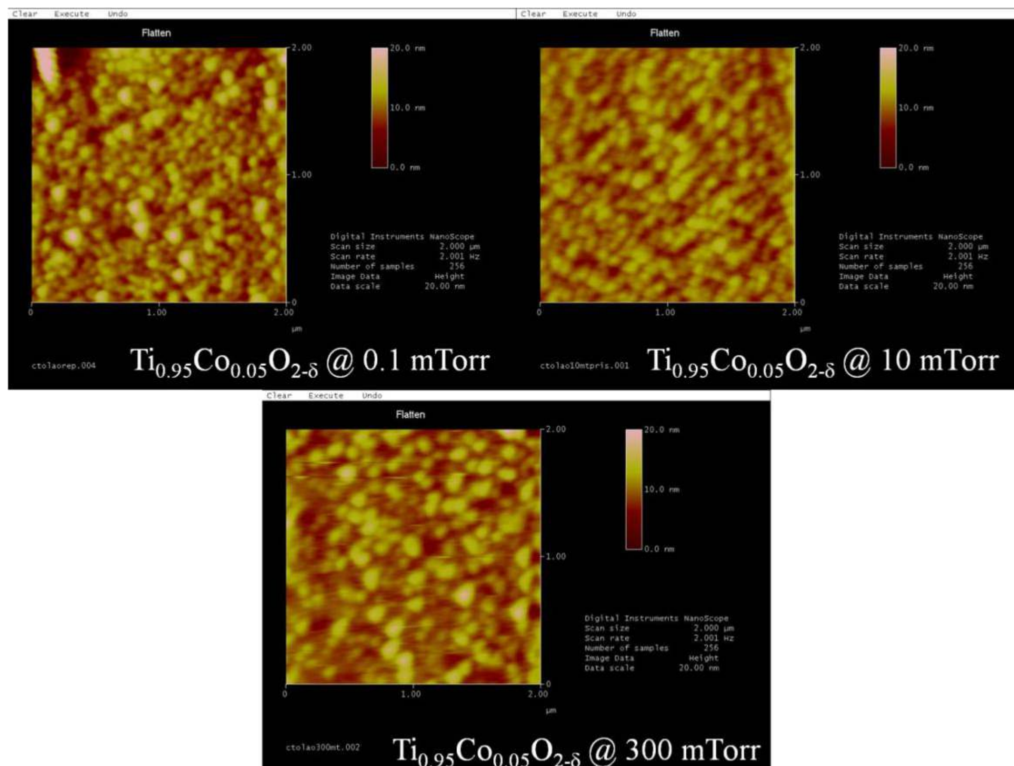

Fig.5.12 SPM images of $Ti_{0.95}Co_{0.05}O_{2-\delta}$ films deposited on $LaAlO_3$ at (a) 0.1 mTorr, (b) 10 mTorr and (c) 300 mTorr oxygen partial pressure.

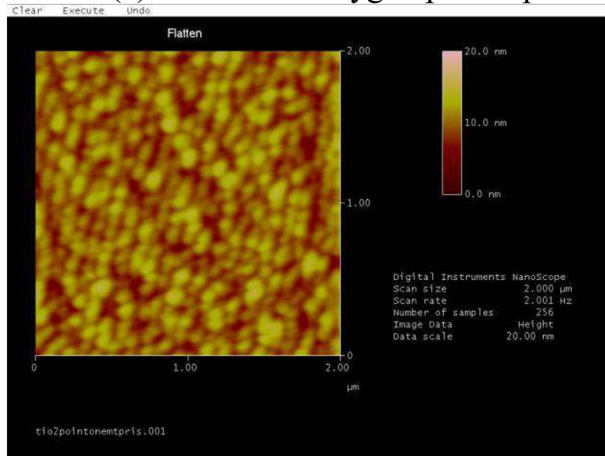

Fig.5.13 A typical SPM image of $TiO_{2-\delta}$ film deposited at 0.1 mTorr oxygen partial pressure.

5.3 Magnetic Properties of $Ti_{1-x}Co_xO_{2-\delta}$ Films Deposited on Si and $LaAlO_3$ Substrate

The magnetisation (M) versus applied magnetic field (H) shows hysteresis behaviour in all films at 300 K (Fig.5.14 (a) and (b)). The M vs. H

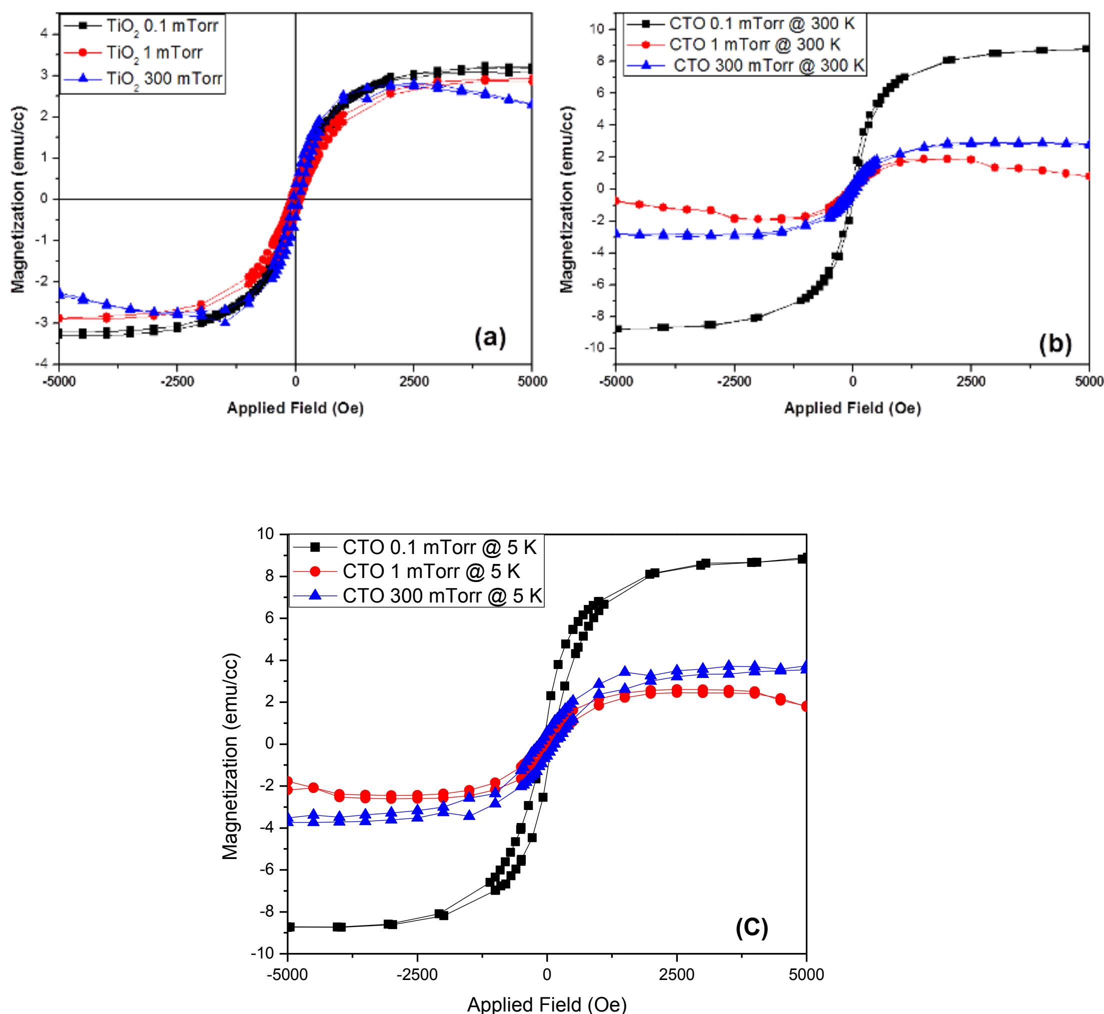

Fig.5.14 Magnetisation (M) vs. applied magnetic field (H) of: (a) TiO_2 film deposited at 0.1 mTorr, 1mTorr and 300 mTorr (at 300 K) (b) CTO films deposited at 0.1 mTorr, 1 mTorr and 300 mTorr oxygen partial pressure (at 300 K) and (C) CTO films deposited at 0.1 mTorr, 1 mTorr and 300 mTorr oxygen partial pressure (at 5 K).

loop of TiO_2 and CTO films deposited on Si substrate at various oxygen partial pressures at room temperature are shown in Fig.5.14 (a) and (b) respectively. The hysteresis persists in the films down to 5 K. Fig. 5.14 (c) shows M vs. H. loops of the CTO films and measured at 5 K.

Rumaiz et al. (2007) have observed the RTFM in TiO_2 film deposited at 0.2 mTorr of oxygen partial pressure and diamagnetic behaviour in film

deposited at 50 mTorr. However, in our case, RTFM persists in both TiO_2 and CTO films even deposited at 300 mTorr oxygen partial pressure. In addition, we have shown saturation magnetisation (M_S) in TiO_2 thin films have 1 to 2 order of magnitude higher than the magnetisation reported by Rumaiz et al. (2007) where Si substrate has been used in both cases. Compared to TiO_2 cluster films, M_S is also found to be more than an order of magnitude higher in our case [Wei et al. (2009)]. In CTO films, the magnetisation is found to be increased with decrease in oxygen partial pressure as reported in case of Cr doped TiO_2 thin films [Zhang et al. (2008)].

For $Ti_{1-x}Co_xO_{2-\delta}$ films deposited on $LaAlO_3$ substrates, the magnetisation as a function of temperature under ZFC and FC condition with a probing field of 50 Oe are depicted in Fig.5.14 (a). The retention of the bifurcation in M_{ZFC} and M_{FC} upto 300 K, suggest that T_C is above room temperature. From Fig.5.14 (a), it is clear that the difference between M_{FC} and M_{ZFC} decreases with increasing oxygen partial pressure. Similar bifurcation in M_{ZFC} and M_{FC} has been observed for the TiO_2 thin films deposited at various oxygen partial pressures. A typical M vs. T plot for the TiO_2 film deposited at 0.1 mTorr oxygen partial pressure has been shown in Fig.5.14 (b). The magnetisation as a function of applied magnetic field at 300 K is depicted in Fig.5.15.

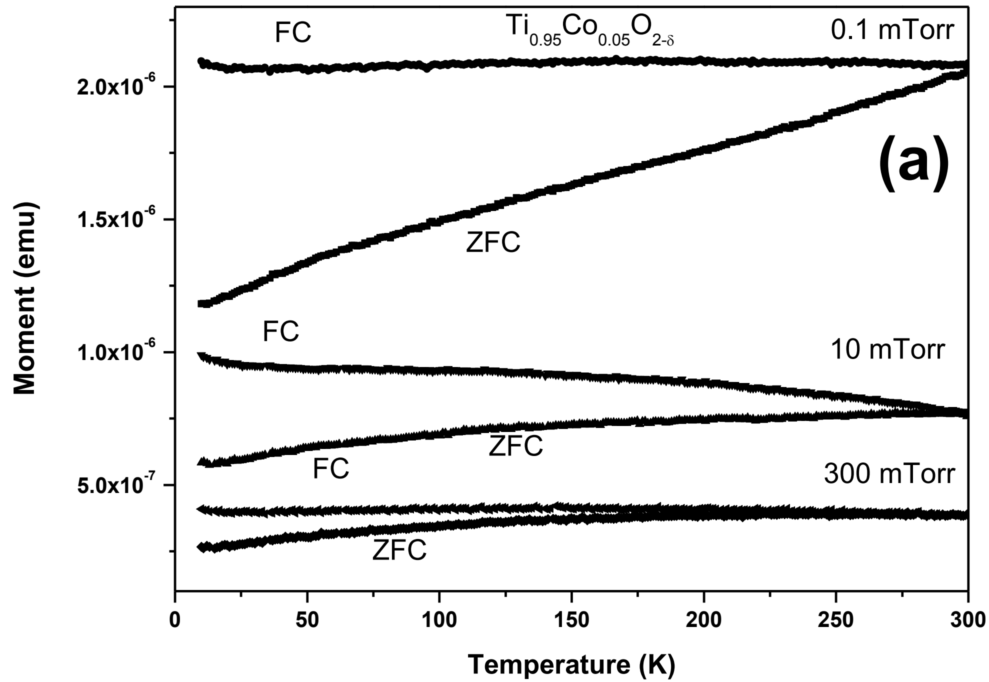

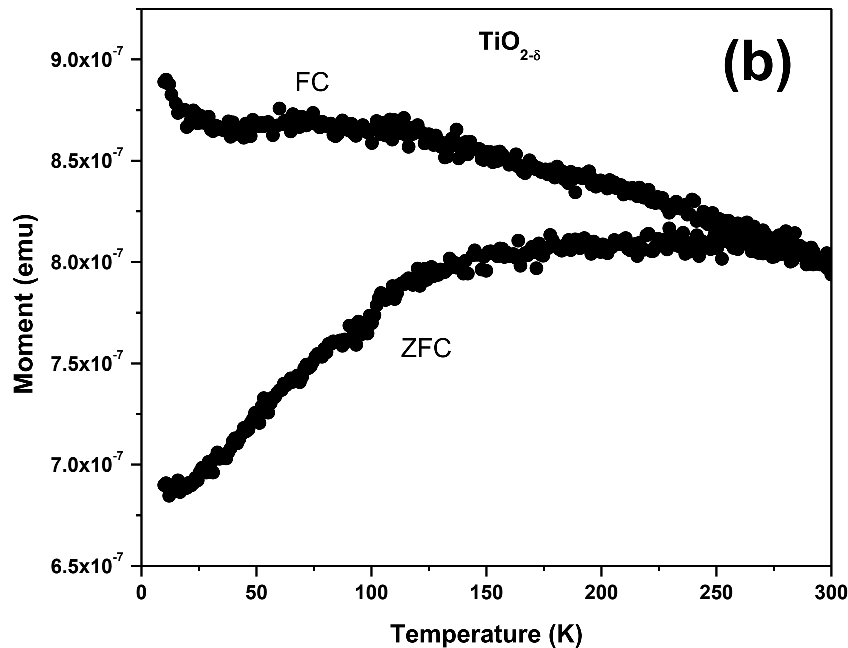

Fig.5.15 ZFC and FC magnetisation (M) vs. temperature (T) at 50 Oe of (a) CTO films deposited at 0.1 mTorr, 1 mTorr and 300 mTorr oxygen partial pressures (b) TiO_2 films deposited at 0.1 mTorr oxygen partial pressure.

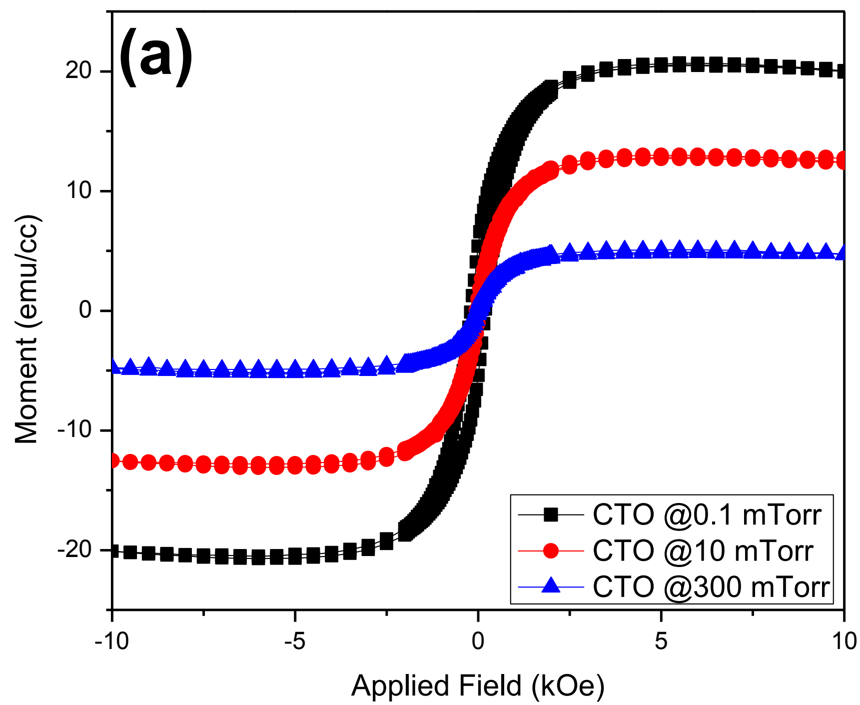
(a)
20
10
0
-10
-20
Moment (emu/cc)
-10
-5
0
5
10
Applied Field (kOe)
CTO @0.1 mTorr
CTO @10 mTorr
CTO @300 mTorr

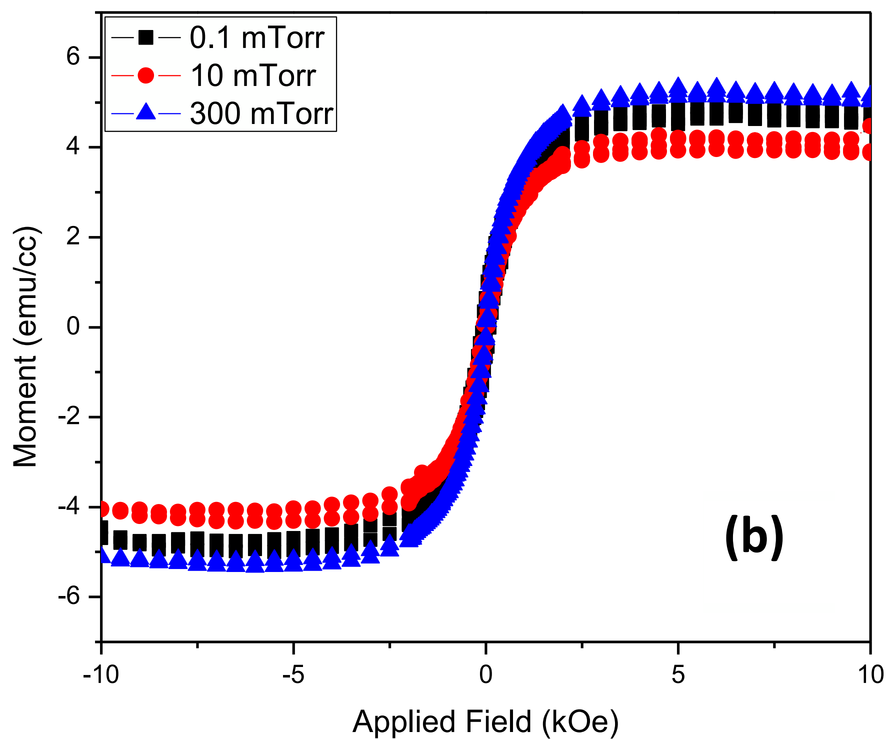
0.1 mTorr
10 mTorr
300 mTorr
6
4
2
0
-2
-4
-6
Moment (emu/cc)
(b)
-10
-5
0
5
10
Applied Field (kOe)

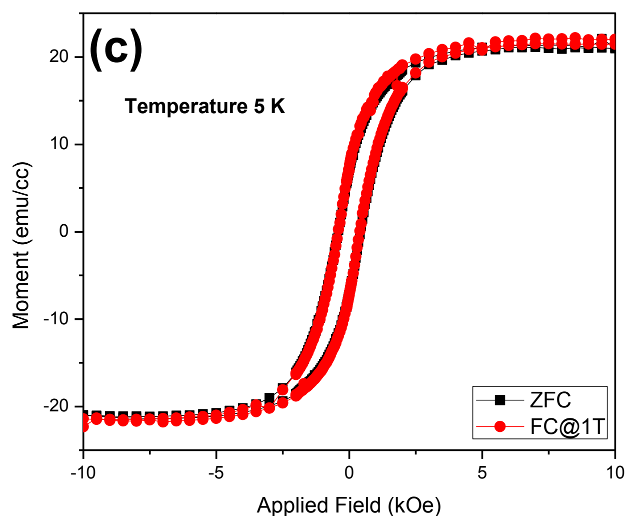

Fig.5.16 Magnetisation (M) vs. applied magnetic field (H) at 300 K of (a) CTO (b) TiO_2 films deposited at 0.1 mTorr, 1mTorr and 300 mTorr. (c) A typical M vs. H plot for CTO film deposited at 0.1 mTorr oxygen partial pressure under ZFC and FC condition.

The magnetisation of $Ti_{1-x}Co_xO_{2-\delta}$ thin films is greatly affected by oxygen partial pressure. The saturation magnetisation M_s decreases from 20 emu/cc to 5 emu/cc with increase in oxygen partial pressure from 0.1 to 300 mTorr (Fig.5.16 (a)). The gradual decrease in M_s corroborates with similar decrease in the difference of M_{FC} and M_{ZFC} as measured from the M vs. T of the same. However, TiO_2 films do not show significant change in saturation magnetisation (Fig.5.16 (b)). In Co-doped TiO_2 films the possibility of Co to form CoO (antiferromagnetic) is quite high, as metallic Co has a tendency to form corresponding oxides. If CoO phase exists, then one may expect the existence of an interface between the antiferromagnetic CoO with T_N ~ 293 K and ferromagnetic phase of the matrix [Pratt Jr and Coelho (1959)] which should show exchange bias. To confirm this, we have performed M vs. H measurement for the CTO film at 5 K under a cooling field of 1 Tesla shown as Fig. 5.16 (c). We do not observe any shift in the hysteresis loop under ZFC and FC conditions thus refutes the possibility of formation of CoO.

5.4 Discussion

There are several reports probing the reasons behind the room temperature ferromagnetic behaviour in both undoped and doped semiconductors like TiO_2, SnO_2, HfO_2 etc. [Matsumato et al. (2001), Ogale et al. (2003), Yamada et al. (2011), Hong et al. (2005), Spaldin (2004), Hong et al. (2006), Yoon et al. (2006), Straumal et al. (2009)]. For example, Wei et al. (2009) show that the oxygen 2p electron plays an important role in the exchange interaction and ferromagnetic ordering. The large overlap between neighboring oxygen 2p orbital ensures an effective interaction range and relatively high ordering temperature, in spite of low net magnetic moment [Wei et al. (2009)]. Sundaresan et al. (2006) report that the electrons trapped in oxygen vacancies (F Centers) are possibly polarized and give rise to RTFM. Theoretical calculations suggest that the oxygen vacancies situated near the transition metals are more stable than that near to titanium. The exchange interaction between the transition metal and oxygen vacancy depends sensitively on the distance between them [Zhang et al. (2008), Jaffe et al. (2005)]. As a consequence, the transition metals are ready to capture the vacancy electrons, which would change the total density of state near the Fermi level and thus result in an enhancement of FM [Zhang et al. (2008)]. If the vacancy is further apart from the transition metal, its influence on the magnetisation would be reduced or diminished eventually [Zhang et al. (2008)]. Kim et al. (2009) report RTFM in both anatase and rutile phases and justify the more magnetic moment in the latter due to more oxygen defects in the distorted TiO_6 octahedra. This is in agreement with our results where pure rutile CTO film deposited at 0.1 mTorr shows four times higher magnetisation than almost anatase CTO film deposited at 300 mTorr on Si substrate. One may note that, in addition to rutile phase in the CTO film deposited at 300 mTorr, film is also highly crystalline compared to the latter one. However, the same argument proposed by Kim et al. (2009) is not followed in TiO_2 film as the

magnetisation in anatase TiO_2 deposited at 300 mTorr is higher than the rutile TiO_2 deposited at 0.1 mTorr.

The magnetism in DMS systems is often raises some conflicting issues. Specially, in case of thin films there are several issues that have to be resolved before concluding the origin of magnetism. In literature, there are reports where magnetism is caused due to intrinsic magnetic contamination of the substrate used for the deposition or adherence of magnetic impurities during the sample preparation [Zhang et al. (2009)]. Also the non-uniform distribution of Co throughout the film lead to the observed magnetism as sometimes these ferromagnetic properties are related to surface of the films. Some suggests non-uniform distribution of Co at the substrate and film interface as a possible source of ferromagnetism which is extrinsic in nature [Shinde et al. (2004)].

We have used Teflon forceps while handling the substrate as well as thin films during deposition. Substrates were cleaned with trichloroethylene, acetone, ethanol and distilled water to remove surface contaminants before deposition. The deposition chamber was also thoroughly cleaned before deposition. To refute the possible intrinsic magnetic contamination of the substrates, we have carried out the M vs. H measurements of the Si and $LaAlO_3$ substrates used in the present experiment. Fig.5.17 (a) and (b) depicts the M-H curves measured at room temperature (300 K) as well as at low temperature (5 K for Si and 1.8 K for $LaAlO_3$). Both Si and $LaAlO_3$ show complete diamagnetic behaviour at 300 K. $LaAlO_3$ substrate shows slight non linearity in the M-H curve measured at 1.8 K whereas Si substrate retains the diamagnetic nature at 5 K.

The M-H curve for the sample holder of the SQUID-VSM including the quartz sample holder with the Teflon surrounding is shown as inset of Fig.5.17 (b). From these experiments, it is clear that neither the substrate nor the sample holder is responsible for the observed ferromagnetism in the $Ti_{1-x}Co_xO_{2-\delta}$ films as discussed earlier.

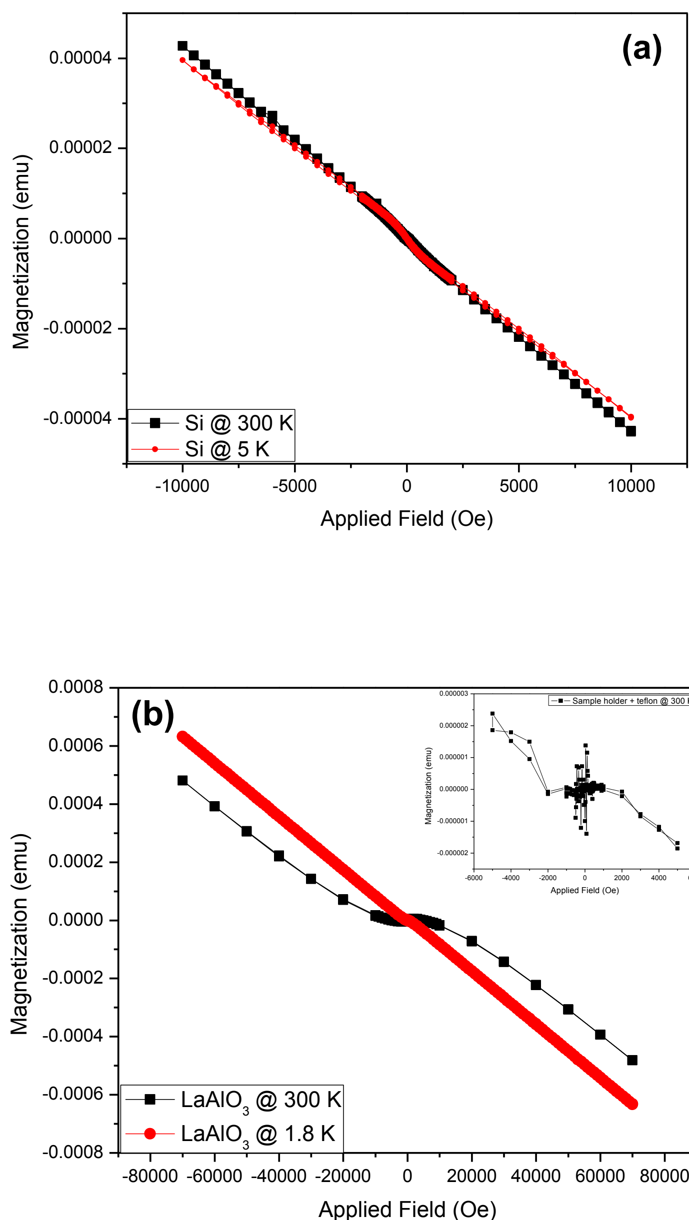

Fig.5.17 Magnetisation (M) vs. applied magnetic field (H) of (a) Si substrate measured at 300 K and 5 K and (b) $LaAlO_3$ measured at 300 K and 1.8 K. Inset of (b) shows the M vs. H plot of the sample holder.

Next, we come to the issue of non-uniform distribution of Co throughout the film as the source of magnetism. XPS is basically sensitive to investigate the oxidation state of the elements present in the surface of the film. Therefore, if any impurity is present in the surface of the film, one can detect it by XPS. Besides Co, one cannot be sure about the content of oxygen below certain

depth of the film. To compare the surface properties with the bulk, we have carried out the depth profiling of a CTO film deposited at 300 mTorr for 40 and 80 minutes by using 2keV Ar^+ ions. Results are shown in fig. 5.18 where we do not observe any remarkable difference in O 1s, Ti 2p and Co 2p regions after argon irradiation.

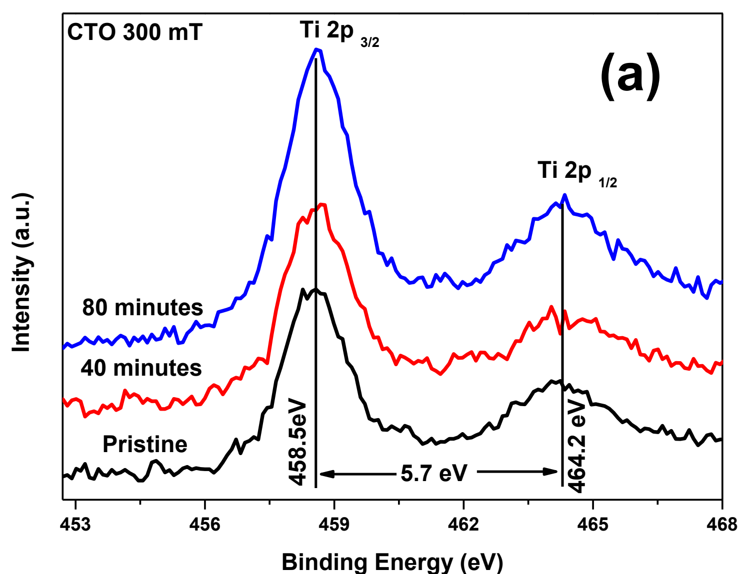

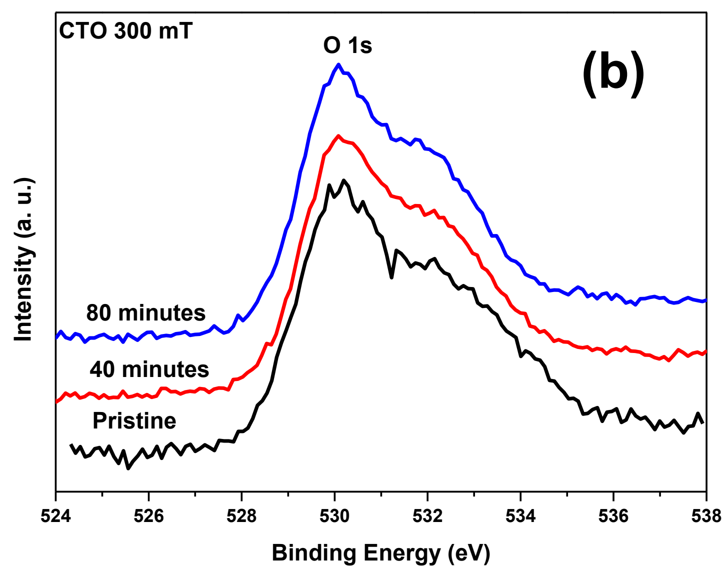

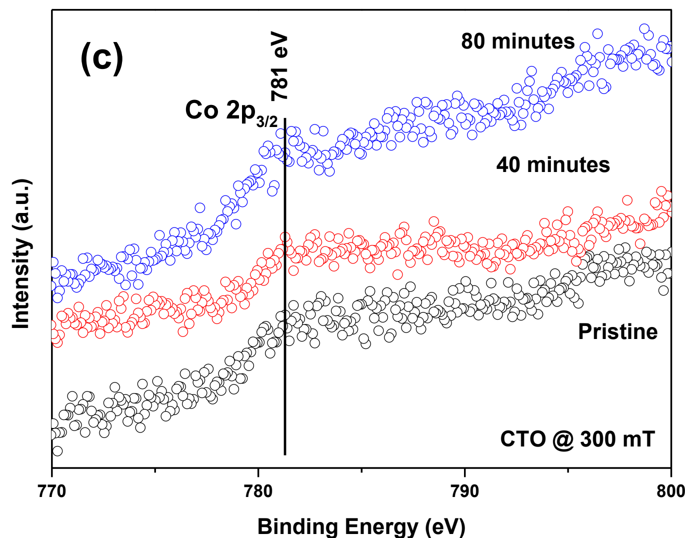

Fig.5.18. XPS Core level spectra of CTO film deposited at 300 mTorr: (a) Ti 2p (b) O 1s and (c) Co 2p region with 2keV Ar^+ ion sputtering for 40 and 80 minutes.

From XPS depth profiling, we believe there is no much difference in surface and bulk properties of these films. Presence of Co clusters on the film surface may give rise to anomalous signal in MFM. Hence, we have confirmed it from the MFM study for CTO films deposited at 0.1 and 1 mTorr oxygen partial pressures on Si substrate.

Fig. 5.19 shows the MFM image of $Ti_{0.985}Co_{0.015}O_{2-\delta}$ film deposited at 0.1 and 1 mTorr oxygen partial pressures on Si substrates. Though the domains are not clear from the MFM results due to small size, but it clearly indicates the ferromagnetic nature of the films. No spurious signal related to clustering of ferromagnetic Co over the film surface has been observed. Qualitatively, we have correlated the RTFM to the RBS results where we have demonstrated that with increase in oxygen partial pressure non-stoichiometry and thickness of the films decrease. At the same time, we have eliminated the factors such as magnetic contamination/impurities resulting into RTFM from XPS depth profiling (Fig.5.18 a-c). We have selected one CTO film deposited on Si substrate for the cross sectional TEM study to check the Co inhomogeneity at

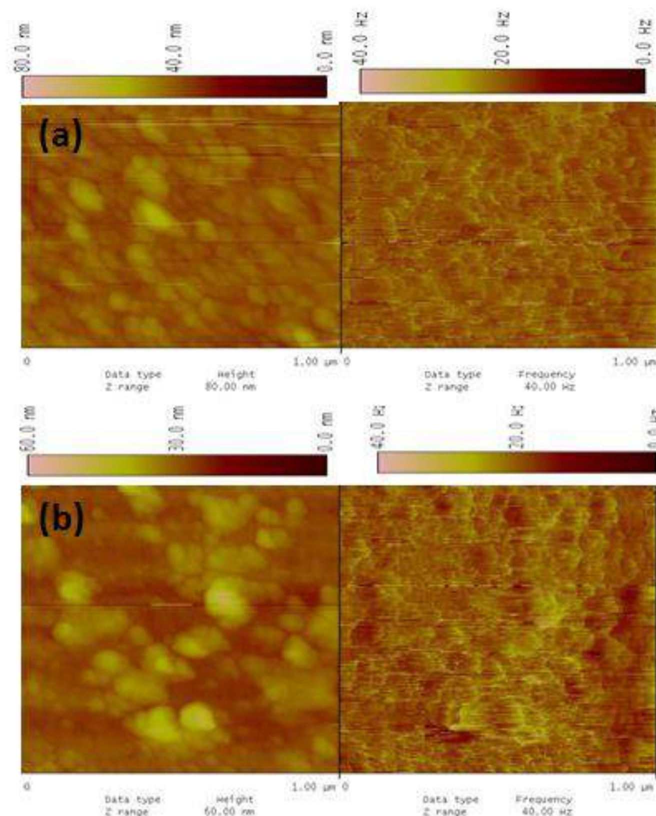

Fig.5.19 Topographic (left panel: $(Height)_{max}$~60 nm) and corresponding MFM image (right panel: $(Height)_{max}$~ 40 Hz) of the film $Ti_{0.985}Co_{0.015}O_{2-\delta}$ deposited at (a) 0.1 mTorr and (b) 1 mTorr oxygen partial pressure.

the interface of film and the substrate (Fig.5.20).

The contamination in the substrate has also been discarded by doing the energy dispersive x-ray spectroscopy (EDS) of the same (Fig.5.21). EDS performed at different locations of the substrate do not show the presence of any foreign element. A typical EDS pattern of the substrate is shown as Fig. 5.21(b). The lattice fringes corresponding to (110) plane of rutile phase of TiO_2 observed in HREM shown as inset of Fig.5.20 reveal good crystallinity and refute the presence of Co clusters supporting the XPS depth profiling results. Our findings are also supported by the reported literatures [Yamada et al. (2011), Shinde et al. (2003)].

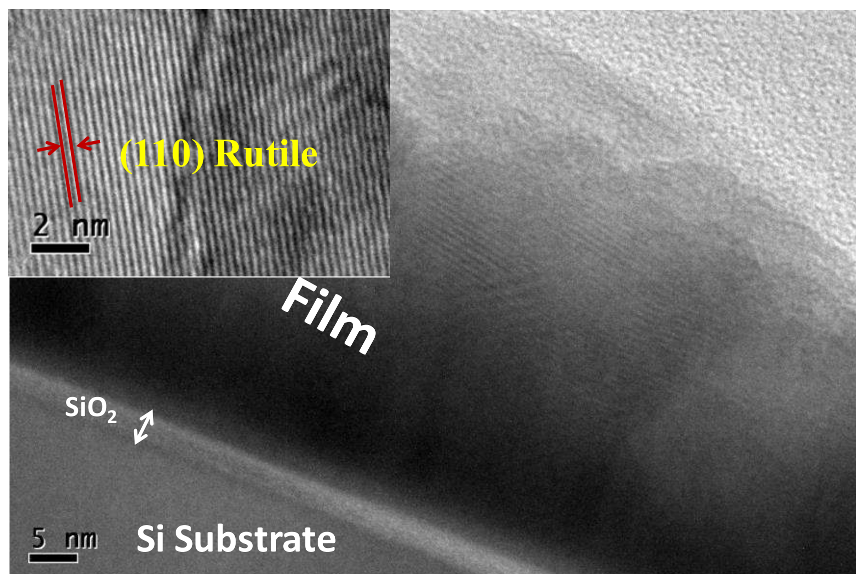

Fig.5.20. A typical high resolution cross sectional transmission electron micrograph of CTO film. Inset shows the high resolution electron microscopic image corresponding to (110) plane of rutile phase of TiO_2.

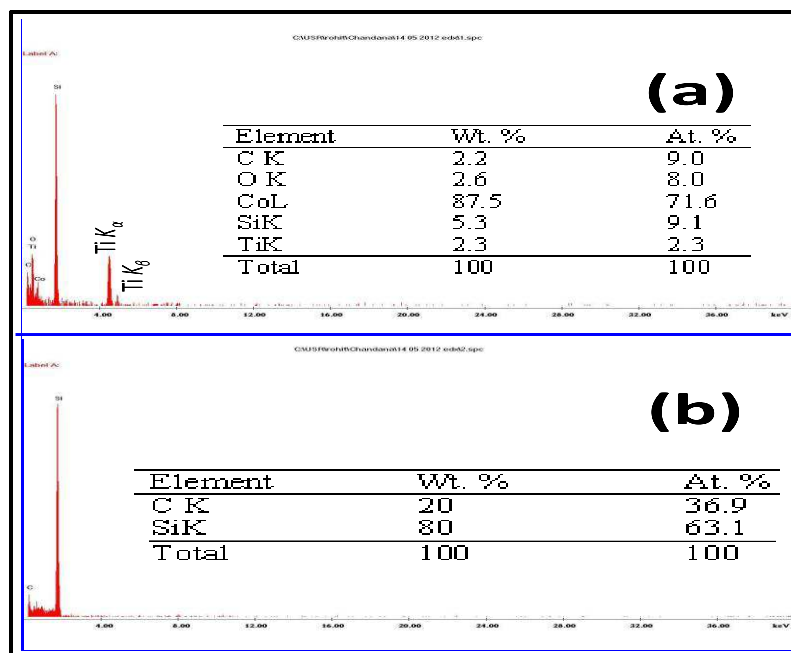

Element	Wt. %	At. %
C K	2.2	9.0
O K	2.6	8.0
CoL	87.5	71.6
SiK	5.3	9.1
TiK	2.3	2.3
Total	100	100

Element	Wt. %	At. %
C K	20	36.9
SiK	80	63.1
Total	100	100

Fig.5.21 Typical EDS spectra recorded over the (a) film and (b) substrate of $Ti_{0.985}Co_{0.015}O_{2-\delta}$ film with elemental compositions as inset.

Yamada et al. (2011) have shown that Co atoms are uniformly distributed without any segregation at the surface or interface in $Ti_{0.90}Co_{0.10}O_2$ film deposited by PLD by bright field scanning transmission electron

microscopy (STEM) imaging and corresponding energy dispersive x-ray spectroscopy mapping of each individual elements. Matusmato et al. (2001) have reported 7 at % of Co in TiO_2 film. As in our case, Co concentration is taken 1.5 and 5 at % that are comparatively less than the aforementioned reports. Therefore, the reason for the observed room temperature ferromagnetism defies the possibility of impurities or contaminations in the present case.

5.5 Summary

We have deposited $Ti_{1-x}Co_xO_{2-\delta}$ thin films on Si as well as $LaAlO_3$ substrate by PLD technique at various oxygen partial pressures. The phase, stoichiometry and morphology of these films are examined by XRD, Raman, RBS and FE-SEM. With increasing oxygen partial pressure while transition from rutile to anatase phase formation observed in TiO_2, CTO film show anatase with small rutile phase at highest oxygen partial pressure i.e. 300 mTorr (for films deposited on Si). It is revealed from XPS that more oxygen vacancies are accommodated in CTO films in comparison to TiO_2 and hence hinders the complete anatase phase formation in CTO film. Magnetic measurements reveal RTFM in all films independent of their phase and substrates. We have confirmed from the cross-sectional TEM and XPS depth profiling measurements that RTFM is neither due to the presence of any contamination/impurities in the substrate nor due to any Co cluster in the film. Further, we have established that in addition to phase, crystallinity of films also play a major role in deciding the magnetic moment in both TiO_2 as well as CTO films deposited on Si substrate. The ferromagnetism is also shown by $Ti_{1-x}Co_xO_{2-\delta}$ (x = 0, 0.05) films deposited on $LaAlO_3$ substrate. However, due to minimum lattice mismatch between the substrate and film, anatase phase retains irrespective of change in oxygen partial pressure. The effect of oxygen partial pressure on magnetic properties of CTO films are clearly seen whereas the variation in M_s is not significant in case of TiO_2 films deposited on the

same substrate under similar deposition conditions. In a nut shell, we observe ferromagnetism in all the films at 300 K irrespective of phase, oxygen partial pressure and substrate without any impurities or contaminations in addition to higher magnetic moment.